Thermochimica Acta, 34 (1979) 133—148

THERMAL EXPANSION COEFFICIENT OF SHEET MOLDING COMPOUND *

C.T. SUN ** and R.G. LENZ

Engineering Mechanics Department, General Motors Research Laboratories, Warren, Michigan 48090 (U.S.A.)

(Received 5 March 1979)

ABSTRACT

The thermal expansion coefficient (TEC) of sheet molding compound (SMC) was determined. The experimental determination was accomplished by measuring directly the changes in length of specimens induced by temperature changes. The theoretical derivation was completed by using existing formulae for unidirectional composites and then applying the averaging procedure to obtain the TEC for randomly oriented chopped-fiber composites (SMC).

Based on the results of this paper, we observed that SMC tested exhibited strong nonhomogeneity and anisotropy. The in-plane TEC was close to that of aluminum, but in the direction normal to the panel was about three times that of aluminum.

INTRODUCTION

During service, an automobile can encounter summer temperatures as high as 50°C and winter temperatures as low as —40°C. These temperature variations might induce high thermal and residual stresses and unacceptable panel deflections if there should be a strong mismatch of linear thermal expansion coefficients of the various interconnecting structural components of the car. Because Sheet Molding Compound (SMC) is being considered for more widespread use in automotive structures, it is desirable to ascertain its thermal expansion characteristics so that such thermal and residual stresses can be taken into account.

A typical SMC consists of three primary phases; chopped glass fibers, polyester resin, and calcium carbonate filler. It will be seen in Table 3 that the coefficients of thermal expansion for polyester are about 15 times higher than those for glass fibers and calcium carbonate filler.

There are two experimental approaches to the measurement of the coefficients of linear thermal expansion. One is to use special strain gages [1,2] made for high temperature applications. Once the thermal strain ϵ_T is known

---

* Presented at the 8th North American Thermal Analysis Society Conference, Atlanta, Georgia, October 16—18, 1978.

** Present address: Department of Engineering Sciences, University of Florida, Gainesville, Florida 32611, U.S.A.

for a given temperature change ΔT, the linear thermal expansion coefficient α is given by

$$\alpha = \frac{\epsilon_T}{\Delta T} \tag{1}$$

Recently, Khayyat [3] employed this technique to measure the coefficient of linear thermal expansion of plastics.

Another method is to use special displacement-field measuring techniques such as the holographic-moire technique [4], the holographic interferometry technique [5—7], and scattered-light speckle-pattern analysis [8,9] to measure the change in length ΔL of a specimen directly. Then the linear thermal expansion coefficient α is given by

$$\alpha = \frac{\Delta L}{L\,\Delta T} \tag{2}$$

where L is the gage length of the specimen.

In this report, we use the second experimental method, adapting one recommended by the American Society for Testing and Materials (ASTM) [10], to measure α experimentally. Details of the experimental set-up are presented in the following sections. The experimental results are compared with numerical values calculated from two theoretical models.

Experimental results show that the stiffness and strength of SMC depend on the direction along which they are measured [11—12]. Therefore, it was hypothesized that the coefficient of linear thermal expansion of SMC might also be direction-dependent. In the following experiments, we measure α of SMC-45 and SMC-55 (45 and 55 wt.% of glass fiber) along three orthogonal directions, two in the plane of the panel and one normal to the plane of the panel. In order to see further how α varies with direction in the plane of the panel, we also measured α along six different directions for one specimen (SMC-55E3). It was assumed that the in-plane principal axes of the thermal expansion coefficient tensor * are oriented the same all over the plane of the sheet; i.e. they do not rotate from point to point in the plane of the sheet.

EXPERIMENTAL PROCEDURE

Specimen preparation

Eight SMC sheets ranging in nominal thickness from 2.67 mm (0.105 in.) to 5.84 mm (0.230 in.), and of two compositions (45 and 55 wt.% of glass fiber), were selected for the tests. A list of thicknesses for each glass fiber percentage is shown in Tables 1 and 2. From each molded sheet, a 25.4 mm X 25.4 mm (1 in. X 1 in.) square was cut and finish-ground to size and shape.

* In all the experiments except for specimen SMC-55E3, the in-plane coefficients were measured along the two orthogonal directions parallel to adjacent sides of the square specimens. Measurements of the coefficient along at least three non-coincident directions would have been necessary to ascertain the orientation of the in-plane principal axes (the material axes) with respect to these geometric axes.

TABLE 1

Experimental thermal expansion data for SMC-45

Specimen no.	Average thickness (mm)	α_1(mm mm^{-1} °C^{-1}) × 10^{-6}		α_2(mm mm^{-1} °C^{-1}) × 10^{-6}		α_1/α_2
		Measured value	Most likely error (%)	Measured value	Most likely error (%)	
45A3	2.65	27.23	2.7	21.23	2.8	
45B3	4.20	30.96	2.6	21.23	2.8	
45C3	4.70	14.99	3.0	23.54	2.7	
45D3	5.80	25.31	2.7	24.94	2.7	
Mean value		24.62		22.74		1.08
Standard deviation		5.92		1.58		
Coefficient of variation		24%		7%		

TABLE 2

Experimental thermal expansion data for SMC-55

Specimen no.	Average thickness (mm)	α_1(mm mm^{-1} °C^{-1}) × 10^{-6}		α_2(mm mm^{-1} °C^{-1}) × 10^{-6}		α_1/α_2
		Measured value	Most likely error (%)	Measured value	Most likely error (%)	
55B3	2.60	25.03	2.7	23.38	2.7	
55C3	3.85	23.99	2.7	21.87	2.7	
55D3	4.65	17.61	2.9	11.86	3.3	
55E3	5.80	25.89	2.7	15.27	3.0	
Mean value		23.13		18.10		1.28
Standard deviation		3.26		4.72		
Coefficient of variation		14.1%		26%		

Fig. 1. Finished test samples.

For the multi-directional expansion measurement, a 55% glass fiber, 5.38 mm (0.212 in.) thick sheet was selected. From this sheet a 12-sided equiangular polygon (dodecagon) was cut and finish-ground to 25.4 mm (1.00 in.) across opposite sides.

The sheet-thickness expansion measurement was made on 55 wt.% glass fiber SMC. Five pieces, each approximately 9.5 mm (0.38 in.) square, were cut from this material, ground flat on the faces to minimize waviness, stacked into a sandwich, and one piece further ground so that the total sandwich thickness of the five pieces was 25.4 mm (1.00 in.). The pieces were simply stacked together without adhesives.

These specimens are shown in Fig. 1.

Fixture build-up and test method

Our familiarity with high-sensitivity displacement probes led us to select an electronic displacement probe and meter for the thermal expansion measurements. Figure 2 shows the oven (door open) in which the specimens were placed; the fan for circulating the air inside the oven is visible in the lower center of the photograph. The specimen temperature was increased from ambient temperature to 93.3°C (200°F) in four discrete steps, with specimen temperature monitored by an attached, shielded iron/constantan thermocouple. To detect thermal expansion of the heated specimens, one end of an Invar rod * was placed against the upper surface of the test piece, through a small hole in the oven ceiling, to a sensitive probe resting against a reference surface on top of the oven. (For detail, see the sketch shown in Fig. 5, below.)

Prior experience with this type of heating device indicated that positional instability of the interior oven surfaces was a major problem, particularly in view of the minute dimensional changes expected and the accuracy required. To eliminate this inherent structural instability, an external, adjustable straight-line datum reference was used for our probe, to allow dimensional changes to be detected only in the plane of the datum, the direction of the traverse of the probe; thus, any minor tilting of the specimen with respect to this plane would not affect the measurements. To eliminate specimen-tilt measuring effects within the datum plane, the specimen was placed between two Invar rods of equal length, the lower ends of the rods resting against the base on which the specimen rested (see the photograph, Fig. 2, and the sketch, Fig. 5); the upper ends of these two rods thus indicated the position of the specimen base with reference to the plane of the datum. Prior to each measurement the upper ends of these two Invar rods were made parallel (zeroed) with the datum by adjusting the tilt of the datum surface. (The upper ends of the Invar rods, the contact probe, and the vertically adjustable reference surface are shown in Fig. 3. A close-up view of the rods and probe

* Invar, a registered trademark of the International Nickel Company for a special nickel-based alloy, has a thermal expansion coefficient of $1.3 \times 10^{-6}°C^{-1}$ [13], an order of magnitude less than that of most common structural materials, and thus introduced minimal error to the thermal displacement measurement.

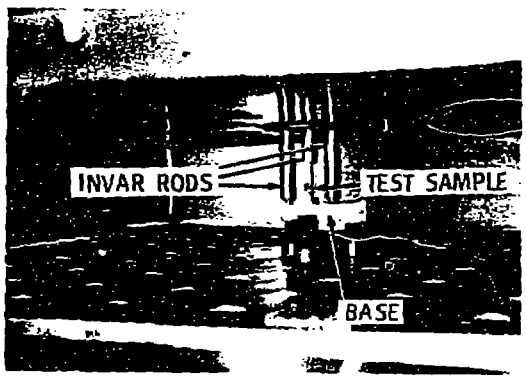

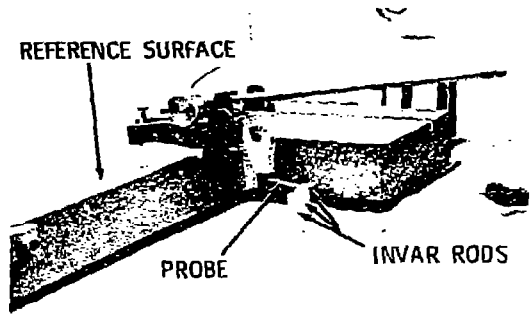

Fig. 2. Interior view showing test sample, base, and Invar rods.

Fig. 3. Over-top surface showing tops of Invar rods, probe and adjustable reference (datum) surface.

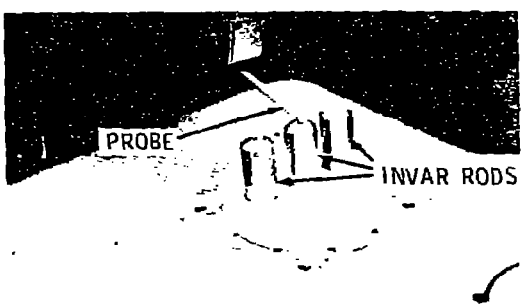

Fig. 4. Close-up of probe and tops of Invar rods.

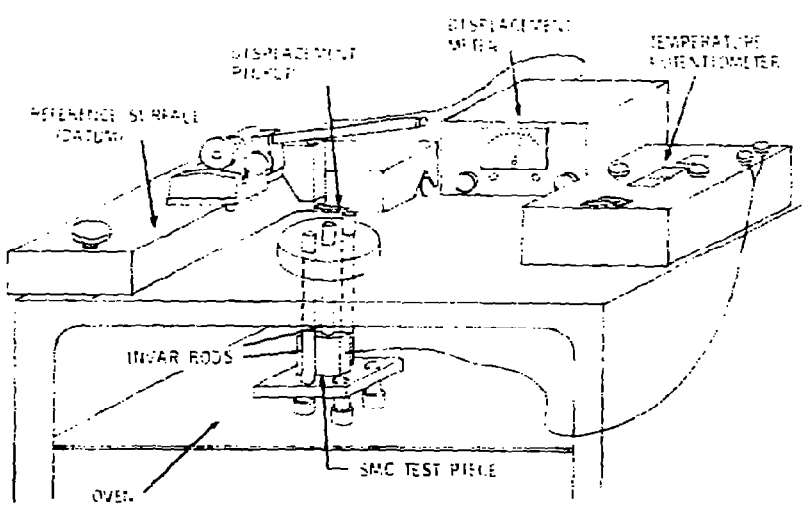

Fig. 5. Sketch of measurement set-up.

is shown in Fig. 4.) This adjustment minimized the effect of specimen tilt on the expansion measurements.

In this manner, the probe readings of the Invar rod in contact with the specimen were consistently made perpendicular to the specimen base, and unaffected by any slight tilting o the base resulting from temperature changes in the oven. Holes were drilled in an aluminum plate in the oven ceiling to support the three Invar rods. The two reference rods were 9.5 mm (3/8 in.) in diameter and 152 mm (6.00 in.) long. The test-sample rod was the same diameter but 25.4 mm (1.00 in.) shorter. A sketch of the entire set-up is shown in Fig. 5.

Preliminary verification

To determine the stability of the reference (datum) surface during an 8 h measurement cycle, the specimen was replaced by an Invar bar of specimen length and of a composition similar to that used in the two reference rods. Thus, three Invar columns of equal length extended from the base surface through the oven ceiling to the contact probe. Expansion measurements (ΔL) were taken at each of four approximately equal steps over the temperature range from 23°C (74°F) to 92°C (200°F). After the reference surface was realigned with the two outer reference rods, no change in reading was detected [to within a measuring sensitivity of 1.2 μm (50 μin.)] when measuring the center rod, at any of the four temperature steps. This confirmed that the reference (datum) surface did not measurably distort over the temperature cycle.

As a check on the entire system, a 25.4 mm (1.00 in.) square block of 6.4 mm (1/4 in.) thick aluminum alloy, 2024-T, was measured for thermal expansion over a 71°C (128°F) temperature range, to compare with the published value of α. It was not intended as a calibration procedure. The average of three tests resulted in a value of $25 \times 10^{-6}°C^{-1}$ ($13.9 \times 10^{-6}°F^{-1}$) for the unit expansion. This compares with a published value of $23.2 \times 10^{-6}°C^{-1}$ ($12.9 \times 10^{-6}°F^{-1}$) for this alloy [14]. This determination took into account the thermal expansion of the different length Invar rods.

Measurements

Prior to each test, an iron/constantan thermocouple was inserted into a tight-fitting hole drilled centrally into one side of each test piece as shown in Fig. 5. The depth of insertion was greater than 10 times the thermocouple diameter to minimize possible conduction errors along the thermocouple axis. The thermocouple was held in place by the snug fit between the hole and the thermocouple. The thermocouple was connected to a Leeds and Northrup temperature potentiometer, Model 8692, Serial Number 1571772, outside the heating chamber. Thermocouple and potentiometer were calibrated at the GM Research Laboratories by standardized calibration methods at 22.9°C (73.2°F), 42.4°C (108.3°F), and 91.1°C (204.9°F); the maximum error at these temperatures was +0.3°C (0.6°F). The displacement probe, a Mitutoyo electronic gage head mounted on a toolmakers' surface gage, was

set up with the surface-gage base on the positioning table. This table became the reference datum for the electronic gage probe traverse across the Invar rod ends. It was adjustable vertically to angular increments of less than 1×10^{-4} unit of vertical movement per unit of length, or 20 seconds of angular arc. The probe was connected to a Mitutoyo electronic gage meter, Model BMA-77, Serial Number 83406 L. This meter had a least-reading capability of 2.54 μm (1×10^{-4} in.) per division, and 7.62 μm ($\pm 30 \times 10^{-4}$ in.) full scale reading.

At the initial ambient temperature, 23°C (74°F), the probe was traversed over the two outer Invar rods, the datum positioning table adjusted to equalize these two readings, and the probe readjusted to give a zero meter reading. At this condition, the probe was located over the central Invar rod, and the meter reading and temperature recorded.

The temperature control on the oven was then reset approximately 16.7°C (30°F) higher. After this temperature was reached and allowed to stabilize for about two hours, the datum table was adjusted and expansion and temperature readings taken as described above. This process was repeated for four 16.7°C (30°F) intervals until the temperature reached 93°C (200°F), and readings recorded at each interval. The entire test cycle took one working day.

For the multi-directional tests on the dodecagonal specimen, the procedure described above was followed for each of the six pairs of opposite sides.

For the thickness-expansion test of the five-layer sandwich, the specimen was placed between the two reference Invar rods, and the measurement rod lowered to contact the top of the test-specimen stack. No cement or glue was used between layers. The heating cycles and expansion and temperature recording used in the earlier tests were repeated.

The thermal expansion coefficient was calculated by dividing the difference between the meter reading of the zero-reference Invar rod and the reading of the Invar rod in contact with the SMC specimen, by the temperature difference, as shown in eqn. (2). This calculated value was corrected for the different lengths of Invar bars by adding to it the expansion coefficient of Invar (1.3×10^{-6}°C^{-1}) multiplied by the difference in Invar-bar lengths (25.4 mm).

To determine firstly whether there were any significant hysteresis-producing effects inherent in the heat-up test method and then whether any changes occurred in the thermal expansion characteristics of the SMC because of prolonged exposure to the elevated test temperature, a temperature-reversal (or thermal contraction) test was performed. Sample 45-D3 was heated to 93°C (200°F) and held at this temperature overnight. Measurements were then made at four temperature decrements taken at two-hour intervals. These temperatures corresponded to those of the previous tests. The contraction-test results are shown at the end of the section of charts in Fig. 10, plotted with the corresponding expansion-test data. We observe from this plot that there is no apparent change in expansion properties by this prolonged exposure at the elevated temperatures encountered in these tests, nor is there any appreciable hysteresis effect resulting from rate- or thermal-lag effects.

Measurement error

The displacement-measurement error was calculated to be no larger than the sum of the calibration error and the meter reading uncertainty. The meter reading uncertainty was estimated as one-quarter of a meter division, or 0.63 μm (0.000 025 in.). The calibration error, by actual test on the GMR Micro Motion Calibrator *, was linear — 2.5% over the full scale of 150 μm (0.006 in.). As an example, with a change in meter reading of 26 divisions, a typical value, the error would be 2.5% of 26 divisions plus 0.25 divisions, for a total of 0.90 divisions. Since each division was 2.5 μm (0.0001 in.), the estimated maximum error is 2.25 μm (0.000089 in.). This error expressed as a percentage of the meter reading is 0.90/26 or 3.5%. The RMS error, calculated as the square root of the sum of the squares of the percentage errors, is 2.7%. For larger meter-reading intervals (larger expansions) this percentage error decreases.

The error in the Invar expansion coefficient for the measured length correction in this case causes less than 0.025 μm (1×10^{-6} in.) difference in corrected values and is negligible.

DISCUSSION OF DATA

Figure 6 shows a typical plot of ΔL as a function of the temperature T for speciment SMC-45A3. For other specimens, the relations between ΔL and T are almost identical to specimen SMC-45A3 shown in Fig. 6. In order to reduce the length of the paper, these figures are omitted; but the numerical results are tabulated in Tables 1 and 2 for specimens SMC-45 and SMC-55, respectively. From Fig. 6, we observe that, within the temperature range tested, ΔL is almost a linear function of the temperature T. This implies that the coefficient of linear thermal expansion (the slope of the ΔL vs. T curve divided by the specimen gage length L) is nearly constant over that temperature range. Tables 1 and 2, summarizing the test results in the plane of the panel, show considerable scatter from specimen to specimen. With the exception of α along the y direction of SMC-45, all the coefficients of variation, which indicate the degree of scattering, exceed 10%. These variations are shown in Fig. 7 for SMC-45 and SMC-55. This means that, in order to have reliable design data, a statistically significant number of specimens should be tested.

Based on the limited number of specimens tested, α is lower for the SMC containing the larger percentage of glass fibers. This is physically reasonable since the glass, having a much higher Young's modulus (E), dominates the deformation of the composite, and its thermal expansion coefficient is much lower than that of resin.

It is also interesting to observe from Tables 1 and 2 that the ratio of α_1

* See The Design, Calibration, and Operation of a Micro-Displacement Device, Paper No. 13.1, 1965, 20th Annual Instrument Society of America Conference, October 4—7, 1965, Los Angeles, California.

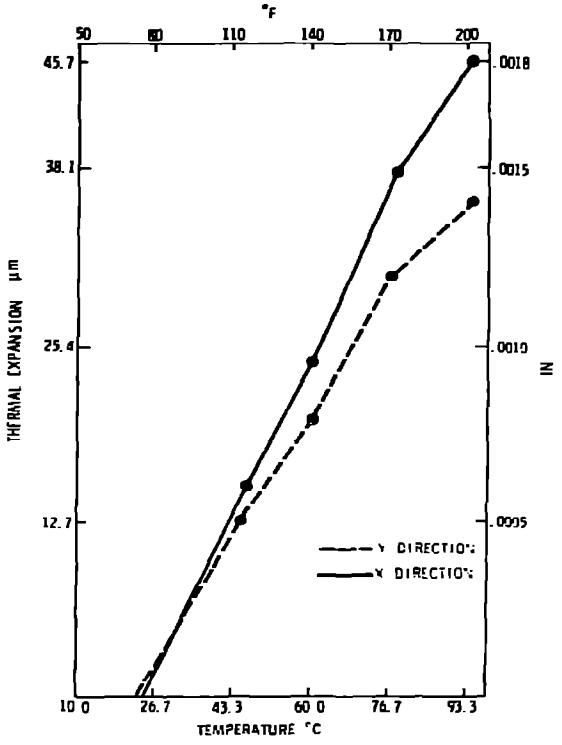

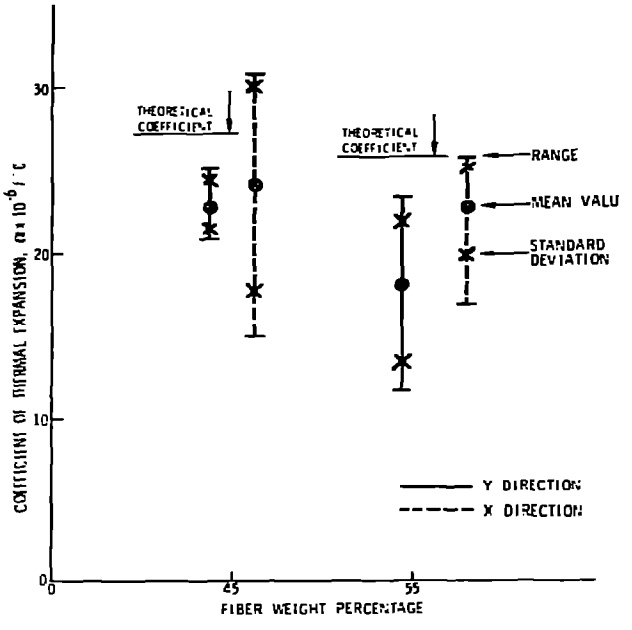

Fig. 6. Plot of ΔL vs. T for specimen 45-A3.

Fig. 7. Plot of range of in-plane test values for α.

and α_2 is 1.09 for SMC-45 and 1.32 for SMC-55. This ratio is an indication of the degree of anisotropy * of the material. Thus SMC-55 appears to be more anisotropic than SMC-45, but a more detailed examination would be necessary to establish this. Again, based on the limited number of specimens, the experimental results seem to indicate that the degree of anisotropy increases as the fiber content increases, although it is probably related also to the degree of deformation induced during molding [15].

Figure 8 shows the experimental values of the linear thermal expansion coefficient for SMC-55E3 along six directions differing by 30° increments. The maximum value ($24.2 \times 10^{-6°} C^{-1}$) is about the same as the value for the x direction, and the minimum value ($15.3 \times 10^{-6°} C^{-1}$) coincides with the value for the y direction. Now let us pass a "best fit" imaginary ellipse through the data points (i.e. the mid-points of the arcs representing the data on Fig. 8) to represent the magnitude of the α-tensor in the various directions. The minimum and maximum radii (representing the principal axes) are mutually orthogonal, of course; more significantly, they are oriented

* As noted in the earlier footnote discussing the choice of axes, the axes chosen might not have been principal axes with respect to the thermal expansion tensor. Thus the actual ratio of the principal coefficients will be at least as large as that found in these experiments.

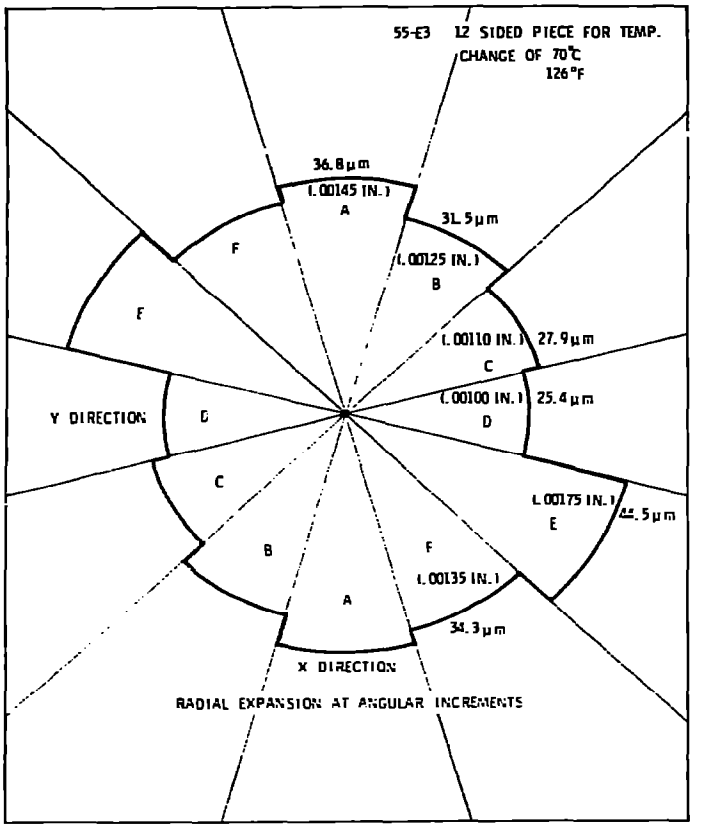

Fig. 8. Plot of ΔL as a function of the angular direction.

approximately 30° counterclockwise relative to the "geometrically convenient" axes (the x and y axes) indicated on the figure. While the numerical values of the α_{ij} obtainable from this ellipse representing the α-tensor might not be useful because of the limited number of data points used in constructing the ellipse and apparent scatter (cf. points A, F, and E), its rotation relative to the x and y axes strongly suggests that the geometric axes indicated are indeed not the principal axes of the α-tensor.

Experimental data for the thermal expansion along the direction normal to the panel (thickness direction) is shown in Fig. 9 for SMC-55E3, from which the linear thermal expansion coefficient was calculated to be $73.3 \times 10^{-6°}C^{-1}$. This result is also consistent with physical intuition: since the fibers lie in the plane of the panel, along the direction normal to the panel there is less constraint for expansion and contraction due to temperature change than along directions in the plane of the panel. The coefficient of linear thermal expansion normal to the plane is thus dominated by the matrix material (i.e. the polyester resin). This explains why the thermal expansion coefficient along the thickness direction is more than three times the in-plane values.

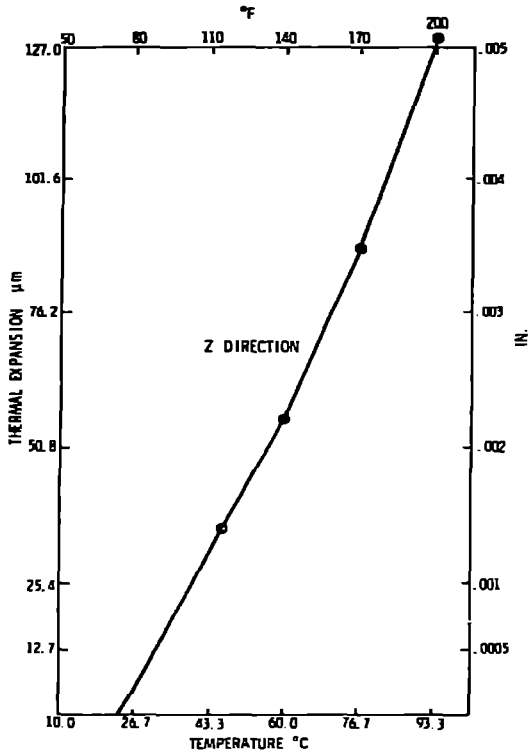

Fig. 9. Plot of ΔL vs. T along thickness direction for specimen 55-E3.

THEORETICAL PREDICTION

For randomly oriented chopped-fiber composites, Eisenberg [15] showed that elastic properties such as the elastic moduli are related to the corresponding property of a unidirectional composite having all fibers oriented in the ϕ direction, by the following relation

$$\bar{p}(\lambda) = \frac{\lambda}{\pi} \int_0^{\pi} \frac{p(\phi)}{1 + (\lambda^2 - 1)\sin^2\phi} \, d\phi \tag{3}$$

where $\bar{p}$ represents any elastic property of a randomly oriented chopped-fiber composite, $p(\phi)$ represents the same property of a unidirectional composite having all fibers oriented in the ϕ direction and λ ($\lambda \geqslant 1$) is the stretch ratio of SMC due to molding. Suppose that the thermal expansion coefficients follow the same relation as the elastic moduli. Thus we have

$$\bar{\alpha}_1(\lambda) = \frac{\lambda}{\pi} \int_0^{\pi} \frac{\alpha_1'(\phi)}{1 + (\lambda^2 - 1)\sin^2\phi} \, d\phi \tag{4}$$

$$\bar{\alpha}_2(\lambda) = \frac{\lambda}{\pi} \int_0^{\pi} \frac{\alpha_2'(\phi)}{1 + (\lambda^2 - 1)\sin^2\phi} \, d\phi \tag{5}$$

$$\bar{\alpha}_6(\lambda) = \frac{\lambda}{\pi} \int_0^{\pi} \frac{\alpha_6'(\phi)}{1 + (\lambda^2 - 1)\sin^2\phi} \, d\phi \tag{6}$$

where α_1', α_2', and α_6' represent the coefficients of in-plane thermal expansion and in-plane angular distortion of a unidirectionally reinforced composite having all fibers oriented in the ϕ-direction. The relations between $\alpha_i'(\phi)$ and the longitudinal and transverse thermal expansion coefficients of a unidirectionally reinforced composite are obtained from the tensor transformation formula

$$\begin{aligned}
\alpha_1'(\phi) &= \alpha_L \cos^2\phi + \alpha_T \sin^2\phi \\
\alpha_2'(\phi) &= \alpha_L \sin^2\phi + \alpha_T \cos^2\phi \\
\alpha_6'(\phi) &= (\alpha_T - \alpha_L) \sin\phi \cos\phi
\end{aligned} \tag{7}$$

where α_L and α_T represent respectively the longitudinal (along the fiber) and the transverse (perpendicular to the fiber) thermal expansion coefficients of a unidirectionally reinforced fiber composite.

Substituting $\alpha_i'(\phi)$ from eqn. (7) into eqns. (4)—(6) and carrying out the integration, we obtain

$$\begin{aligned}
\bar{\alpha}_1(\lambda) &= \frac{\lambda\alpha_L + \alpha_T}{1 + \lambda} \\
\bar{\alpha}_2(\lambda) &= \frac{\alpha_L + \lambda\alpha_T}{1 + \lambda} \\
\bar{\alpha}_6(\lambda) &\equiv 0
\end{aligned} \tag{8}$$

Equations (8) show that for randomly oriented chopped-fiber composites, the two in-plane thermal expansion coefficients are not equal unless $\lambda = 1$ and $\bar{\alpha}_6$ is identically zero. When $\lambda > 1$, the two coefficients differ because of the preferential orientation of the fibers.

When the fibers remain randomly oriented, $\lambda = 1$ and we have

$$\bar{\alpha}_1 = \bar{\alpha}_2 = \tfrac{1}{2}(\alpha_L + \alpha_T) \tag{9}$$

Since the value of λ is unknown for the specimens being tested, we evaluate $\bar{\alpha}_L$ and $\bar{\alpha}_T$ for values of λ varying from 1 to 5. The reason for choosing 5 as the upper bound for λ is that, in practice, 5 is a reasonably maximum stretch [15].

In summary, the theoretical prediction of the in-plane thermal expansion coefficients $\bar{\alpha}_1$ and $\bar{\alpha}_2$ for SMC is given by eqns. (8) where

$$\alpha_L = \frac{E_m(1 - V_f)\alpha_m + E_f V_f \alpha_f}{E_m(1 - V_f) + E_f V_f} \tag{10}$$

$$\alpha_T = (1 + \nu_m)\alpha_m(1 - V_f) + (1 + \nu_f)\alpha_f V_f - \alpha_L[\nu_f V_f + \nu_m(1 - V_f)] \tag{11}$$

The formulae for α_L and α_T given in eqns. (10) and (11) were originally derived by Schapery [16] for unidirectionally reinforced fiber composites.

To evaluate $\bar{\alpha}_1$ and $\bar{\alpha}_2$, we first have to know α_m, α_f, E_m, E_f, ν_m, and ν_f for a given value of V_f. Since the matrix material is a two-phase composite

material with polyester as the resin and calcium carbonate as the filler (assumed to be spherical inclusions), we use the formula derived by Kerner [17] to calculate α_c;

$$\alpha_c = \alpha_i V_i + \alpha_r V_r + \frac{4G_r}{K_c}\left[\frac{K_c - K_i}{4G_r + 3K_i}(\alpha_r - \alpha_i)V_i\right] \tag{12}$$

where the subscript c denotes the composite (in the present case, the filled matrix material), i the inclusion material (calcium carbonate), and r the resin material (polyester). Also, G denotes the shear modulus, K bulk modulus, and K_c the bulk modulus of the filled matrix. It can be calculated from Kerner's derivation [17]

$$K_c = \left(\frac{K_i V_i}{3K_i + 4G_r} + \frac{K_r V_r}{3K_r + 4G_r}\right) \Big/ \left(\frac{V_i}{3K_i + 4G_r} + \frac{V_r}{3K_r + 4G_r}\right) \tag{13}$$

The evaluation of E_m and ν_m in eqns. (10) and (11) comes from a formula similar to eqn. (13) by Kerner [17], in which the shear modulus G_c for the filled matrix was given in terms of G_i, G_r, V_i, etc. Since the filled matrix is presumably an isotropic material, E_m and ν_m can be calculated from the standard relation in terms of K and G.

The values of E, α and ν for each constituent material are given in Table 3 [18—19]. Based on the data given in this table, we first evaluate the corresponding properties of the filled matrix material. The results are given in Table 4. Using eqns. (10) and (11) and the values of E_m, ν_m and α_m, we can evaluate α_L and α_T for SMC-45 and SMC-55, respectively. The results are given in Table 5. Finally, with the values α_L and α_T and eqn. (8), we can evaluate $\bar{\alpha}_1$ and $\bar{\alpha}_2$ as a function of the stretch ratio λ. The results are shown in Table 6. Comparing the experimental results from Tables 1 and 2 with the theoretical prediction, we observe that the theoretical prediction of $\bar{\alpha}_1$ and $\bar{\alpha}_2$ is much higher than the experimental data for the case $\lambda = 1$, and the theoretical value of $\bar{\alpha}_2$ much higher than the experimental value for the cases $\lambda = 2$—5.

The above derivation was based on a model which treats the thermal expansion coefficients as elastic moduli, or stiffnesses. In another sense, they might be acting as compliances, for they are the constants of proportional which relate the resulting strain to the applied "force", (namely, the temper-

TABLE 3

The values of Young's modulus, Poisson's ratio and the coefficient of thermal expansion for each constituent material

	Resin (polyester)	Filler (calcium carbonate)	Fiber (glass)
Young's modulus, E (GPa x 10^6 psi)	3.24 (0.47)	41.4 (6.0)	72.4 (10.5)
Poisson's ratio, ν	0.45	0.21	0.22
Coefficient of thermal expansion, α	85.5 x 10^{-6} °C^{-1} (47.5 x 10^{-6} °F^{-1})	5.04 x 10^{-6} °C^{-1} (2.8 x 10^{-6} °F^{-1})	5.04 x 10^{-6} °C^{-1} (2.8 x 10^{-6} °F^{-1})

TABLE 4

The values of Young's modulus, Poisson's ratio and the coefficient of thermal expansion of the filled matrix material

	E_m (GPa x 10^6 psi)	ν_m	α_m	
			$\times 10^{-6}\,^\circ C^{-1}$	$\times 10^{-6}\,^\circ F^{-1}$
SMC-45	13.45 (1.95)	0.39	62.6	34.8
SMC-55	10.14 (1.47)	0.41	70.2	39.0

TABLE 5

Values of the longitudinal and transverse thermal expansion coefficients for SMC-45 and SMC-55 calculated from eqns. (10) and (11)

	α_L		α_T	
	$\times 10^{-6}\,^\circ C^{-1}$	$\times 10^{-6}\,^\circ F^{-1}$	$\times 10^{-6}\,^\circ C^{-1}$	$\times 10^{-6}\,^\circ F^{-1}$
SMC-45	20.0	11.1	52.2	29.0
SMC-55	15.59	8.66	54.83	30.46

TABLE 6

Values of $\bar{\alpha}_1$ and $\bar{\alpha}_2$ for SMC-45 and SMC-55 as a function of the stretch ratio, λ

	λ	$\bar{\alpha}_1$		$\bar{\alpha}_2$	
		$\times 10^{-6}\,^\circ C^{-1}$	$\times 10^{-6}\,^\circ F^{-1}$	$\times 10^{-6}\,^\circ C^{-1}$	$\times 10^{-6}\,^\circ F^{-1}$
SMC-45	1	36.2	20.1	36.2	20.1
	2	30.8	17.1	41.4	23.0
	3	28.1	15.6	44.1	24.5
	4	26.5	14.7	45.7	25.4
	5	25.4	14.1	46.8	26.0
SMC-55	1	35.3	19.6	35.3	19.6
	2	28.6	15.9	41.8	23.2
	3	25.4	14.1	45.2	25.1
	4	23.6	13.1	47.0	26.1
	5	22.1	12.3	48.4	26.9

ture differential) and so differ from the elastic moduli, acting instead as reciprocal moduli. Pursuing this line of reasoning, let us begin with eqn. (3), substituting $\bar{\alpha}_1$ for p, to get

$$\frac{1}{\bar{\alpha}(\lambda)} = \frac{\lambda}{\pi} \int_0^{\pi} \frac{1}{\alpha'(\phi)[1 + (\lambda^2 - 1)\sin^2\phi]}\, d\phi \tag{14}$$

By substituting eqn. (7) into eqn. (14) and carrying out the integration, we

obtain for the case of $\lambda = 1$

$$\frac{1}{\bar{\alpha}_1} = \frac{1}{\bar{\alpha}_2} \approx \frac{2}{\sqrt{(4\alpha_T - 3\alpha_L)\alpha_L}} \tag{15}$$

Using the values of α_L and α_T for SMC-45 and SMC-55, respectively, and substituting into eqn. (15) one obtains

$$\bar{\alpha}_1 = \bar{\alpha}_2 = 27.3 \times 10^{-6}\ °C^{-1} = 15.2 \times 10^{-6}\ °F^{-1} \tag{16}$$

for SMC-45 and

$$\bar{\alpha}_1 = \bar{\alpha}_2 = 25.9 \times 10^{-6}\ °C^{-1} = 14.4 \times 10^{-6}\ °F^{-1} \tag{17}$$

for SMC-55, when $\lambda = 1$.

The theoretical results based upon eqn. (3) are much higher than the experimental values. If we calculate α from eqn. (14), however, the results are much closer for the case of $\lambda = 1$. The theoretical values of α as shown in eqns. (16) and (17) are also plotted in Fig. 10 with the range of experimental data. Although there is no clear-cut physical basis as to which formula (3) or (14) should be used, the experimental data supports the theoretical results based on eqn. (14).

The theoretical prediction for the thermal expansion coefficient along the thickness direction should be the same as that along the transverse direction, α_T. For SMC-55 the calculated value is $54.8 \times 10^{-6°}C^{-1}$ ($30.5 \times 10^{-6°}F^{-1}$), compared with an experimental value of $73.3 \times 10^{-6°}C^{-1}$ ($40.7 \times 10^{-6°}F^{-1}$). This difference may be due to one or more of the following.

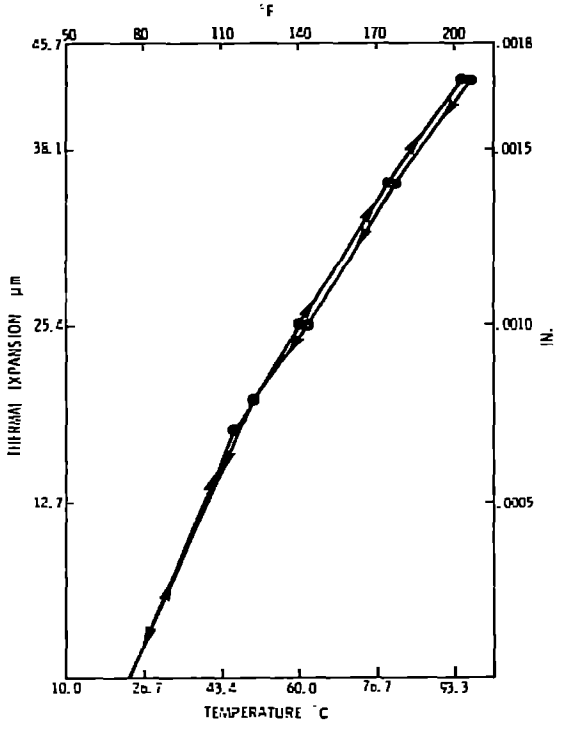

Fig. 10. Comparison of expansion and contraction cycles for specimen 45-D3.

(1) Insufficient experimental data (only one sample was tested).
(2) Inaccuracy of the theoretical model.
(3) Inaccuracy in experimental procedure for the α determination in the thickness direction.

ACKNOWLEDGEMENTS

The authors wish to thank Gil Lalonde for selecting the measuring instruments and environmental chamber, machining the parts and fixture elements, setting up tests, making the measurements, and recording the data. The authors also wish to thank Bill Justusson for suggesting this problem and the model leading to eqn. (14), and David Chang for obtaining the SMC material for testing.

REFERENCES

1 W.N. Sharpe, Jr., Exp. Mech., 15 (1975) 482.
2 O.L. Gillette, Exp. Mech., 15 (1975) 316.
3 F.A. Khayyat, J. Phys. E, 10 (1977) 451.
4 C.A. Sciammarella and J.A. Gilber, Exp. Mech., 16 (1976) 215.
5 T.R. Hsu and R. Lewak, Exp. Mech., 16 (1976) 182.
6 R.C. Sampson, Exp. Mech., 10 (1970) 313.
7 S.K. Dhir and J.P. Sikora, Exp. Mech., 13 (1973) 323.
8 D.B. Barker and M.E. Fourneg, Exp. Mech., 16 (1976) 209.
9 R.L. Johnson, Exp. Mech., 16 (1976) 201.
10 Standard test method for coefficient of linear thermal expansion of plastics, American National Standard ANSI/ASTM D 696-70, American National Standards Institute.
11 C.T. Sun, Mechanical properties of glass fiber reinforced composite and ABS, General Motors Res. Lab. Rep., to be published.
12 J.K. Bard and G.G. Warner, Mold charge pattern versus isotropy of chopped glass/polyester (SMC) panels, General Motors Res. Rep. No. MD 76-018, September 1976.
13 Technical Data Sheet, Carpenter Free-Cut Invar 36, Carpenter Steel Company, Reading, Pennsylvania, January 1963.
14 Alcoa Aluminum Handbook, Aluminum Company of America, Pittsburg, Penrsylvania, 1959.
15 M.A. Eisenberg, Prediction of elastic constants of chopped-fiber/resin panels with molding-induced anisotropy, General Motors Res. Lab, Rep. EM-327, June 1977.
16 R.A. Schapery, J. Compos. Mater., 2 (1968) 380.
17 E.H. Kerner, Proc. Phys. Soc. London, Sect. B, 69 (1956) 808.
18 J.E. Ashton, J.C. Halpin and P.H. Petit, Primer on Composite Materials: Analysis, Technomic Publication, Stamford, Connecticut, 1969, p. 107.
19 R.J. Roark and W.C. Young, Formulas for Stress and Strain, McGraw Hill, New York, 5th edn., 1975, p. 609.